JOURNAL OF SOLID STATE CHEMISTRY 112, 255–261 (1994)

Structure and Optical Conductivity of Silver Thiogermanate Glasses

E. I. Kamitsos,[1] J. A. Kapoutsis, and G. D. Chryssikos

Theoretical and Physical Chemistry Institute, National Hellenic Research Foundation, 48 Vass. Constantinou Ave., Athens 11635, Greece

and

G. Taillades, A. Pradel, and M. Ribes

Laboratoire de Physicochimie des Materiaux Solides, Universite de Montpellier II, URA CNRS D0407, Place E. Bataillon, 34095 Montpellier Cedex 5, France

Received September 23, 1993; accepted December 2, 1993

Silver thiogermanate glasses $x\text{AgI}\cdot(1-x)[y\text{Ag}_2\text{S}\cdot(1-y)\text{GeS}_2]$ were investigated by infrared reflectance and Raman spectroscopies to study the glass structure as a function of Ag_2S ($0 \le y \le 0.5$) and AgI ($y = 0.5$, $0 \le x \le 0.375$) content. The results for binary glasses indicate that addition of Ag_2S to GeS_2 glass induces the depolymerization of the thiogermanate network by creation of terminal Ge–S^- bonds. AgI was also found to affect the network structure and this was expressed by disproportionation reactions. The interactions between Ag^+ ions and their sites were also investigated and discussed in relation to the high ionic conductivity of these glasses. Broad range conductivity spectra were also obtained by combining dielectric and far-infrared conductivity data. © 1994 Academic Press, Inc.

1. INTRODUCTION

In recent years, the search for glasses with high ionic conductivity has led to the preparation of alkali and silver chalcogenide glasses (1–7). The conductivity of such superionic glasses exceeds that of the corresponding oxide systems by as much as three orders of magnitude. It has been proposed that this difference is due primarily to the higher polarizability of sulfide and selenide ions as compared to that of the oxide ion (5, 6). The large glass transition temperature decrease of sulfide glasses was considered also to be a key factor for the increase of the ambient temperature conductivity (8).

The ionic conductivity of silver thiogermanate glasses of the type $x\text{AgI}\cdot(1-x)[y\text{Ag}_2\text{S}\cdot(1-y)\text{GeS}_2]$ has been recently studied over a broad frequency range (1 kHz–10 GHz) as reported elsewhere (9). Yet, the spectrum of ionic movements in glass continues to higher frequencies all the way to the far-infrared, where the oscillations of metal-cations in their localized equilibrium sites are active. As Angell has proposed, the far-infrared conductivity of ionic glasses represents the maximum ionic conductivity attainable at infinitely high temperatures, at which all metal-ion motions become delocalized and contribute to ionic conduction (10, 11). In that respect, we report here the far-infrared optical conductivity of representative silver–iodothiogermanate glasses, which is necessary to complete the ionic conductivity spectrum (9). Moreover, we report results of the infrared and Raman structural study of these glasses and discuss the effect of Ag_2S and AgI additions on the glass structure. The interactions between the mobile Ag^+ ions and their localized sites, as elucidated by the far-infrared absorption spectra, are also discussed in relation to the high ionic conductivity of these glasses.

[1] To whom correspondence should be addressed.

2. EXPERIMENTAL

2.1. Sample Preparation

Binary $y\text{Ag}_2\text{S}\cdot(1-y)\text{GeS}_2$ ($y = 0$, 0.3, 0.4, 0.5) and ternary $x\text{AgI}\cdot(1-x)[0.5\ \text{Ag}_2\text{S}\cdot 0.5\text{GeS}_2]$ ($x = 0$, 0.166, 0.285, 0.375) silver thiogermanate glasses were prepared from reagent grade Ag_2S, GeS_2, and AgI. The stoichiometric batches were thoroughly mixed and placed in silica tubes sealed under vacuum. The mixtures were maintained at 600°C for 2 days to allow solid state reaction. They were subsequently melted at 1000°C and quenched in iced water. Samples for infrared and Raman measurements were obtained by polishing bulk glass pieces with cerium oxide of variable particle size (30, 15, 1, and 0.3 μm).

2.2. Spectral Measurements

Infrared reflectance spectra were measured at room temperature on a Fourier-transform vacuum spectrometer

0022-4596/94 $6.00

(Bruker 113v), by utilizing an 11° off-normal specular reflectance attachment and a high reflectivity aluminum mirror as reference. Each spectrum was measured in the range 30–4000 cm^{-1} with 2 cm^{-1} resolution and represents the average of 200 scans. Absorption and optical conductivity spectra were obtained by Kramers–Kronig (KK) transformation of the reflectance spectra as described elsewhere (12).

Raman spectra were measured on a Ramanor HG 2S Jobin–Yvon spectrometer, using for excitation the 514.5 nm line of a Spectra Physics argon ion laser (~50 mW). All spectra were recorded at room temperature, with a 90° scattering geometry and 5 cm^{-1} resolution.

Experimental details concerning the electrical conductivity measurements in the range 1 kHz–10 GHz are reported elsewhere (9).

3. RESULTS

3.1. Spectra of $yAg_2S \cdot (1 - y)GeS_2$ Glasses

The infrared reflectivity spectra of binary silver thiogermanate glasses are shown in Fig. 1. The spectrum of the GeS_2 glass compares quite well with that reported by Lukovsky *et al.* (13). Addition of Ag_2S appears to reduce drastically the intensity of the reflectivity peak at ca. 360 cm^{-1} and cause its broadening. Such a decrease of reflectivity upon modification was recently observed in alkali borate glasses and was attributed to the increase of the glass molar volume (12b). This appears to be also the case for $yAg_2S \cdot (1 - y)GeS_2$ glasses, since addition of Ag_2S increases the glass molar volume (3), and thus decreases the concentration of the thiogermanate structural groups.

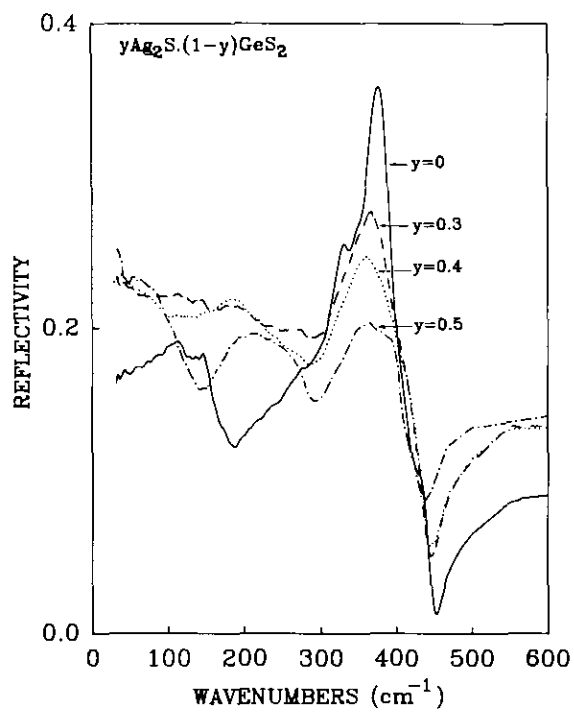

FIG. 1. Infrared reflectivity spectra of $yAg_2S \cdot (1 - y)GeS_2$ glasses.

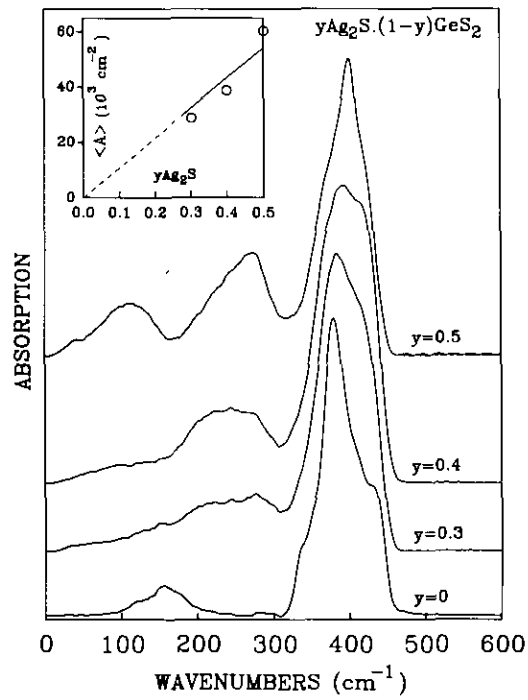

FIG. 2. Infrared absorption spectra of $yAg_2S \cdot (1 - y)GeS_2$ glasses. Inset shows the composition dependence of the integrated intensity of the ca. 100 cm^{-1} band.

The effect of Ag_2S on the glass structure is also demonstrated by the absorption coefficient spectra (Fig. 2), calculated by the KK analysis of the reflectivity spectra. The high frequency envelope centered at ca. 377 cm^{-1} ($y = 0$) becomes broader and changes gradually in shape, while a new asymmetric absorption band develops between 200 and 300 cm^{-1}. In the low frequency part of the spectra a new feature appears at ca. 100 cm^{-1}, peaking eventually at 110 cm^{-1} for $y = 0.5$. The integrated absorption of this band ($\langle A \rangle$) obtained by standard deconvolution techniques (12), is shown in the inset of Fig. 2 as a function of the Ag_2S mole fraction. The linear dependence of the integrated intensity on y suggests that the ca. 100 cm^{-1} band should be attributed to vibrations of Ag^+ ions in their anionic environments (sites) (12).

The Raman spectra of the binary glasses were also measured and are presented in Fig. 3. With the exception of GeS_2 ($y = 0$) the rest of the samples exhibited excess scattering at low frequencies, which greatly reduces the quality of the spectra. Nevertheless, the effect of Ag_2S on glass structure is clearly demonstrated. Thus, the main peak at 342 cm^{-1} ($y = 0$) is reduced in relative intensity, while new bands at ca. 415 and 400 cm^{-1}, in addition to those at ca. 235 and 265 cm^{-1}, grow in intensity with Ag_2S

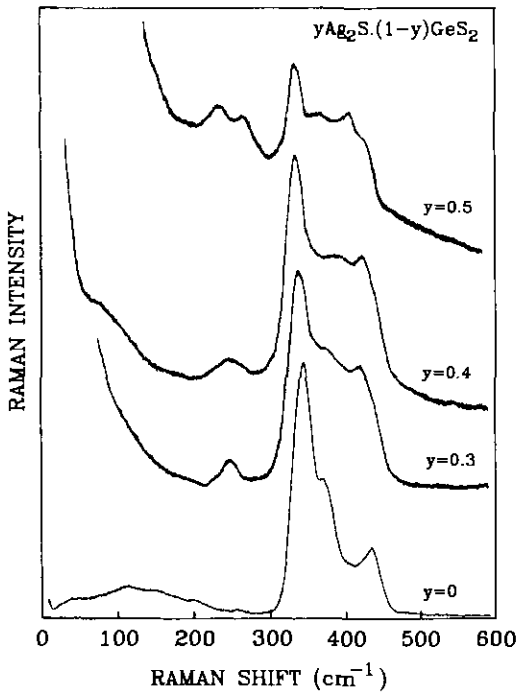

FIG. 3. Raman spectra of $yAg_2S \cdot (1 - y)GeS_2$ glasses.

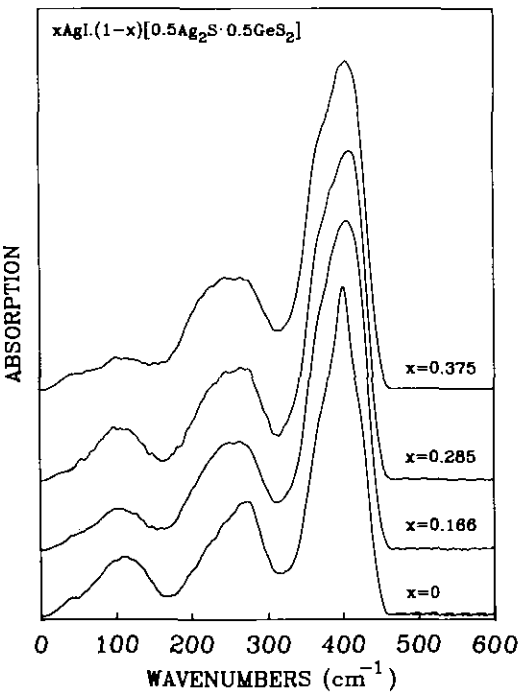

FIG. 4. Infrared absorption spectra of $xAgI \cdot (1 - x)[0.5 Ag_2S \cdot 0.5GeS_2]$ glasses.

content. The last two features were not resolved in the early Raman study of the $y = 0.3$ and 0.5 glass compositions (3). The frequencies of infrared absorption (Fig. 2) and Raman scattering (Fig. 3) maxima are compiled in Table 1.

3.2 *Spectra of* $xAgI \cdot (1 - x)[0.5Ag_2S \cdot 0.5GeS_2]$ *Glasses*

The infrared reflectance spectra of ternary glasses of the composition $xAgI \cdot (1 - x)[0.5Ag_2S \cdot 0.5GeS_2]$ were measured and analyzed in order to investigate the effect

TABLE 1
Assignments of Infrared and Raman Frequencies (cm^{-1}) of Binary $yAg_2S \cdot (1 - y)GeS_2$ and Ternary $xAgI \cdot (1 - x)[0.5Ag_2S \cdot 0.5GeS_2]$ Thiogermanate Glasses

Binary								Ternary			
$y = 0$		$y = 0.3$		$y = 0.4$		$y = 0.5$		$x = 0.09$	$x = 0.166$	$x = 0.231$	
Raman	IR	Raman	IR	Raman	IR	Raman	IR	IR	IR	IR	Assignment
35w				80sh							"boson" band
			70vw,sh		95w		40w,110m	40sh,105m	40sh,105m	45m,105m	Ag^+ motion
110m	115sh		120sh		125w					115m	$\nu_2(E)GeS_{4/2}$
150m	153m		150w							150sh	$\nu_4(F_2)GeS_{4/2}$
200w,sh											
		245w	225m	248w,br	230m	235m	225m	240s	245sh	240s	ν(Ge–S–Ge)di
260vw											
			270m		265m	265m	270s	265s	265s	265s	ν(Ge–S–Ge)meta
					295w,sh				300sh	300sh	ν(Ge–S–Ge)pyro
342vs	340sh	339vs	330w,sh	335vs	325vw,sh	332s					$\nu_1(A_1)GeS_{4/2}$
368s,sh	377vs	375sh	380vs		365sh	370m	365sh	370sh	365sh	370sh	$\nu_3(F_2)GeS_{4/2}$
								380sh.	382sh	385sh	ν(Ge–S^-), pyro
				386br							
					390s	400m	400vs	405s	410s	405s	ν(Ge–S^-)meta
		415m,sh	412s,sh	418m	415sh	420sh	418sh				ν(Ge–S^{-1})di
432s	430s										ν(S–S)

Note. di = $GeS_{2.5}^-$, meta = GeS_3^{2-}, pyro = $GeS_{3.5}^{3-}$, s = strong, m = medium, w = weak, v = very, sh = shoulder.

of AgI on glass structure, while keeping the Ag_2S/GeS_2 ratio fixed. The calculated absorption coefficient spectra are shown in Fig. 4 for variable AgI contents ($x = 0.166$, 0.285, and 0.375) and are compared with that of the 0.5 $Ag_2S \cdot 0.5GeS_2$ binary glass ($x = 0$). It is quite obvious that addition of AgI affects the binary glass spectrum in almost all spectral regions. In particular, the band at ca. 400 cm^{-1} becomes broader at both low and high frequency sides, while the feature between 200 and 300 cm^{-1} develops intensity in the low-frequency side. In addition, the Ag^+-motion band (ca. 100 cm^{-1}) appears to decrease in relative intensity. Attempts to complement the study of the effect of AgI by Raman spectroscopy were not successful due to the strong fluorescence background exhibited by ternary glasses.

4. DISCUSSION

4.1. The Structure of Silver Thiogermanate Glasses

Before discussing the effect of Ag_2S on glass structure it is useful to briefly review the structure and vibrational characteristics of GeS_2 glass, which has been the subject of numerous investigations (13–17). The main vibrational features of this glass can be understood in terms of the modes of $GeS_{4/2}$ tetrahedral "molecules" connected to each other through Ge–S–Ge bridges (13, 14). For tetrahedral point symmetry (T_d) group theory predicts a totally symmetric stretching mode ν_1 (A_1) which is Raman active, an asymmetric stretching mode ν_3 (F_2) which is both IR and Raman active and two bending modes. The first bending mode ν_2(E) is Raman active, while the second one $\nu_4(F_2)$ is both IR and Raman active (Table 2) (18). In that respect, the strong Raman band at 342 cm^{-1} is associated with the ν_1 mode, while the strong infrared feature at 377 cm^{-1}, as well as the Raman shoulder at 368 cm^{-1}, to the ν_3 mode. The ν_2 and ν_4 modes are seen in both infrared and Raman spectra at ca. 115 and 150 cm^{-1}, respectively (Table 1). The infrared activity of ν_2, as well as that of ν_1 (shoulder at ca. 340 cm^{-1}) signifies the presence of intermolecular couplings in the glass (13, 14). In addition to the above features, the Raman spectrum of GeS_2 glass exhibits an additional band at 432 cm^{-1} (430 cm^{-1} in infrared). This band has been attributed to the stretching mode of S–S bonds, which exist at the edges of the interconnected corner-sharing and edge-sharing $GeS_{4/2}$ tetrahedra (16, 17, 19).

Based on the above information we can conclude that the spectra of Fig. 3 indicate the destruction of $GeS_{4/2}$ tetrahedra (reduction of the 342–330 cm^{-1} band intensity) upon addition of Ag_2S. A possible mechanism could involve the rupture of Ge–S–Ge bridges resulting in the formation of terminal $Ge–S^-$ bonds. Evidence for the creation of such nonbridging bonds is manifested by the development of Raman bands at ca. 415 ($y = 0.3$) and 400 cm^{-1} ($y = 0.5$). The results of a comparative Raman study of Na–thiogermanate glasses and crystals (1) suggest that the band at ca. 415 cm^{-1} can be assigned to the stretching vibration of $Ge–S^-$ bonds in dithiogermanate tetrahedra ($GeS^-_{2.5}$), while the one at 400 cm^{-1} to the corresponding mode of metathiogermanate tetrahedra (GeS^{2-}_3) (Table 1). The decrease of the stretching frequency of $Ge–S^-$ bonds upon increasing the number of nonbridging sulfur atoms per germanium tetrahedron is analogous to the behavior of the stretching frequency of $Si–O^-$ bonds in silicate glasses (20, 21).

Creation of $Ge–S^-$ bonds will reduce the T_d symmetry of $GeS_{4/2}$ to at least C_{3v} ($GeS^-_{2.5}$) or C_{2v} (GeS^{2-}_3). Under the new point group symmetries, the symmetric ν_1 Raman modes acquire infrared activity as well, as seen in the correlation table (Table 2). This explains the strong infrared activity at ca. 415 cm^{-1} (dithiogermanate) and 400 cm^{-1} (metathiogermanate) (Fig. 2).

The Raman bands at ca. 230 and 265 cm^{-1} and their corresponding infrared features at similar frequencies can be attributed to a mixed stretching–bending vibration of Ge–S–Ge bridges, ν(Ge–S–Ge), in analogy with silicate glasses (20, 21). The corresponding mode of Si–O–Si bridges is active in the range 430–700 cm^{-1}, depending on the number of non-bridging oxygen atoms per silicon tetrahedron. The frequency of this mode increases with the degree of the network depolymerization (20, 21). On these grounds, we associate the ca. 235 cm^{-1} band with Ge–S–Ge bridges connecting dithiogermanate tetrahedra and the one at ca. 265 cm^{-1} to bridges connecting metathiogermanate tetrahedra. The development of these bands with Ag_2S content parallels that of the bands at ca. 415 and 400 cm^{-1}, attributed also to di- and metathioger-

TABLE 2
Correlation Table for T_d, C_{3v} and C_{2v} Point Group Symmetries

Mode	T_d	C_{3v}	C_{2v}
ν_1	A_1(R)	A_1(R, IR)	A_1(R, IR)
ν_2	E(R)	E(R, IR)	A_1(R, IR) + A_2(R)
ν_3, ν_4	T_2(R, IR)	A_1(R, IR) + E(R, IR)	A_1(R, IR) + B_1(R, IR) + B_2(R, IR)

Note. R and IR denote Raman and infrared activity respectively.

manate tetrahedra, respectively. Therefore, the infrared and Raman spectra show that addition of Ag_2S to GeS_2 glass causes the progressive depolymerization of the thiogermanate network by creation of $Ge–S^-$ terminal bonds. Such bonds have been detected in di- and metathiogermanate tetrahedra in the composition range $0.3 \leq y \leq 0.5$.

The interactions of Ag^+ ions with the thiogermanate network are manifested by the Ag^+-motion band measured at ca. 100 cm^{-1} (Fig. 2). The frequency increase of the absorption maximum with Ag_2S content (Table 1) should be attributed to the increasing anionic charge density of the Ag^+-hosting sulfide sites upon increasing-network depolymerization (22). Besides the main absorption at 110 cm^{-1}, the spectrum of the $y = 0.5$ glass shows the presence of a lower frequency band at (or below) 40 cm^{-1}, which may indicate the presence of different kind of sites of Ag^+ ions (22). It is of interest to note there that the corresponding bands in silver borate glasses were measured at ca. 50 and 180 cm^{-1} (23), suggesting that the Ag^+-oxide interactions are stronger than the Ag^+–sulfide interactions. Such a frequency difference cannot be due entirely to mass effects (24) and thus is taken to indicate a higher decoupling of the Ag^+ motions from the thiogermanate network and therefore to contribute to the higher conductivity exhibited by sulfide glasses.

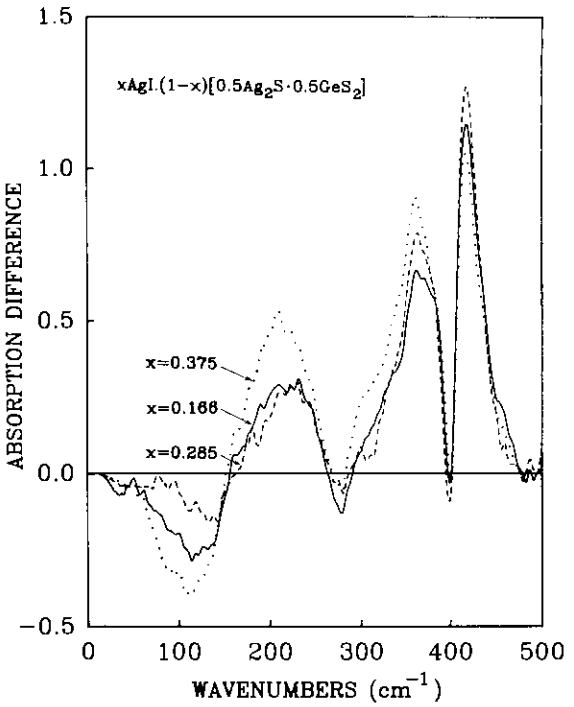

FIG. 5. Infrared difference spectra obtained by subtracting the spectrum of the $0.5Ag_2S \cdot 0.5GeS_2$ glass from those of the ternary $xAgI \cdot (1-x)[0.5Ag_2S \cdot 0.5GeS_2]$ glasses. For details see text.

4.2. Effect of AgI on Glass Structure

On the basis of the above discussion the effect of AgI on the glass structure can now be elucidated. For this purpose difference spectra were calculated by subtracting the spectrum of $0.5Ag_2S–0.5GeS_2$ glass from those of the ternary glasses after scaling at the 400 cm^{-1} band. The results obtained are shown in Fig. 5. Clearly the different spectra show a band at 417 cm^{-1}, an asymmetric profile centred at ca. 365 cm^{-1} with shoulders at 380 and 305 cm^{-1} and negative absorption at ca. 100 cm^{-1}. The band at 417 cm^{-1}, as well as the broad envelope centred at ca. 220 cm^{-1} can be taken as indicating the increasing relative abundance of dithiogermanate tetrahedra in the presence of AgI. Tetrahedra $GeS_{4/2}$ are also formed, as suggested by the asymmetric envelope at ca. 365 cm^{-1}.

Since both $GeS_{4/2}$ and $GeS_{2.5}^-$ (di)tetrahedra are of lowest modification than the meta-(GeS_3^{2-}) stoichiometry, the presence of AgI should also favor the formation of tetrahedra with higher than the metamodification. These are probably the pyrothiogermanate species ($GeS_{3.5}^{3-}$). In Na–thiogermanate glasses the stretching frequency of $Ge–S^-$ bonds is measured at 420 cm^{-1} for meta- and at 400 cm^{-1} for pyrotetrahedra, while in Ag-thiogermanate the frequency of metatetrahedra is at ca. 405 cm^{-1} (Table 1.) Assuming that the same ratio of meta/pyro frequency found in Na glass applies to Ag glasses as well, we estimate a $\nu(GeS^-)$ for pyrotetrahedra at 381 cm^{-1}. The analogy between silicate and germanate glasses can also be employed to estimate the characteristic frequency of Ge–S–Ge bridges connecting pyrotetrahedra. It was shown that metasilicate bridges are characterized by a band at ca. 620 cm^{-1}, while the corresponding band for pyrosilicates appears at ca. 700 cm^{-1} (20, 21). This information together with the fact that metathiogermanate bridges are active at ca. 265 cm^{-1} (Table 1), results in a characteristic frequency at ca. 300 cm^{-1} for pyrothiogermanate arrangements.

Examination of the spectra of Fig. 5 shows the presence of a shoulder at ca. 300 and 385 cm^{-1}, thus giving spectroscopic evidence for the presence of pyrothiogermanate tetrahedra in AgI-containing glasses. These results clearly demonstrate the fact that AgI does influence the structure of the thiogermanate network, in agreement with recent findings in silver–borate glasses containing AgI (23). For the metacomposition ($Ag_2S/GeS_2 = 1$) the present results suggest that AgI favors the disproportionation reactions:

$$3GeS_3^{2-} \rightarrow GeS_{4/2} + 2GeS_{3.5}^{3-}$$

$$2GeS_3^{2-} \rightarrow GeS_{2.5}^- + GeS_{3.5}^{3-}$$

In addition to the species involved in the above equilibria, there is a possibility that mixed germanium iodosulfide

tetrahedra are also formed (19), although the infrared spectra do not confirm their presence in significant quantities.

The effect of AgI is not confined only to the thiogermanate network structure, but it is also manifested on the Ag^+-motion band. As shown in Fig. 4 addition of AgI does not lead to an additional Ag^+-motion band in the far-infrared, but rather to a slight frequency decrease of the main absorption band at ca. 105 cm^{-1}. Considering the fact that the vibration of Ag^+ions in an iodide environment is also active at ca. 100 cm^{-1} (23), this result suggests that, besides sulfide sites, iodide and/or mixed iodosulfide sites hosting Ag^+ ions are created when AgI is added to the binary glass. Of interest is also the result that for $x = 0.375$ the Ag^+-motion band appears to transfer oscillator strength from its high-frequency component (105 cm^{-1}) to the low-frequency one (below 45 cm^{-1}). This observation seems to be quite relevant to the effect of increasing temperature on the far-infrared spectra of α-AgI, which results to the increased absorption at low frequencies (below ca. 60 cm^{-1}) (25, 26). This "extra" absorption was attributed to the disorder of Ag^+ sites, and was thought to characterize superionic conductors (25, 27).

4.3. *The Conductivity Spectrum*

Having established the optical conductivity spectra of Ag–thiogermanate glasses by KK analysis we can now combine these results with lower-frequency conductivity measurements (9), and present a unified conductivity spectrum as suggested first by Wong and Angell (28).

Fig. 6 shows the conductivity spectrum of the ternary glass $0.375AgI \cdot 0.625[0.5Ag_2S \cdot 0.5GeS_2]$ at 300 K. At this temperature, the "dc plateau" of $\sigma = 2 \times 10^{-3}\ \Omega^{-1}\ cm^{-1}$ extends up to ca. 10 MHz. At higher frequencies, $\log \sigma$ increases nonlinearly with $\log f$ and seems to point towards the far-infrared data at 10^{12}–10^{13} Hz. The data of Fig. 6 do not allow the identification of regions with f^1 dependence (28, 29), and power laws with exponents bigger than unity could be also anticipated (30). Moreover, the spectra of AgI-based fast ionic conductors are known to exhibit subTHz features, which are beyond the frequency range of our far-infrared measurements. For example, α-$RbAg_4I_5$ shows a characteristic absorption at 5×10^{11} Hz (ca. 17 cm^{-1}) and a plateau at ca. 10^{11} Hz (30). It is therefore clear that experimental data in the 10^{10}–10^{12} Hz frequency range are needed before definite conclusions on the dynamic profile of Ag^+ motions can be drawn.

5. CONCLUSIONS

The study of the infrared and Raman spectra of $yAg_2S \cdot (1 - y)GeS_2$ glasses has shown that addition of Ag_2S induces the breaking of Ge–S–Ge bridges and the creation of $Ge–S^-$ terminal bonds. Germanium–sulfur tetrahedra with one $Ge–S^-$ bond ($GeS_{2.5}^-$) or two $Ge–S^-$ bonds (GeS_3^{2-}) were detected for Ag_2S contents in the range $0.3 \leq y \leq 0.5$. This shows that Ag_2S behaves as a typical network modifier, in agreement with the results of recent EXAFS studies (31, 32). The increasing network depolymerization with Ag_2S addition is also manifested

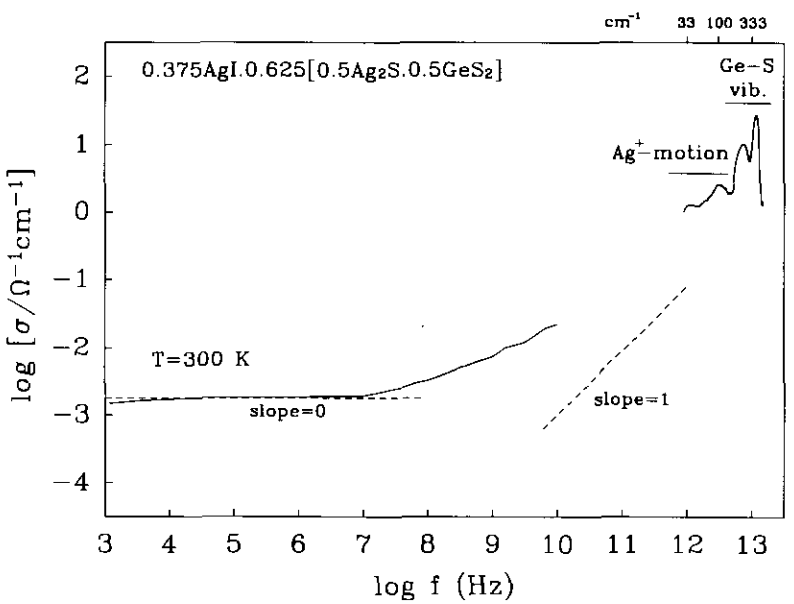

FIG. 6. The conductivity spectrum of the $0.375AgI \cdot 0.625[0.5\ Ag_2S \cdot 0.5GeS_2]$ glass. Measurements in the frequency range 10^{10}–10^{12} Hz are needed to fill the gap.

by an increasing Ag^+-motion frequency, measured between 70 and 110 cm^{-1}.

Addition of AgI to the binary glass $0.5Ag_2S0.5GeS_2$ was found to affect systematically the glass structure. This was expressed by disproportionation reactions which describe the destruction of GeS_3^{2-} tetrahedra and the formation of lower- ($GeS_{4/2}$, $GeS_{2.5}^-$) and higher-modification ($GeS_{3.5}^{3-}$) tetrahedra. At the same time the Ag^+-motion band was found to transfer oscillator strength to lower frequencies (below 40 cm^{-1}), at the expense of the ca. 100 cm^{-1} component. The optical conductivity in the far-infrared was found to point towards the lower-frequency dielectric conductivity data.

ACKNOWLEDGMENT

Collaboration between the two laboratories was supported by the CNRS/NHRF exchange program.

REFERENCES

1. B. Barrau, M. Ribes, M. Maurin, A. Kone, and J. L. Souquet, *J. Non-Cryst. Solids* **37,** 1 (1980).
2. J. L. Souquet, E. Robinel, B. Barrau, and M. Ribes, *Solid State Ionics* **3/4,** 317 (1981).
3. E. Robinel, B. Carette, and M. Ribes, *J. Non-Cryst. Solids* **57,** 49 (1983).
4. H. Eckert, J. H. Kennedy, A. Pradel, and M. Ribes, *J. Non-Cryst. Solids* **113,** 287 (1989).
5. J. M. Reau, B. Tanguy, J. J. Videou, J. Portier, and P. Hagenmuller, *Solid State Ionics* **28–30,** 792 (1988).
6. A. Pradel and M. Ribes, *J. Solid State Chem.* **96,** 247 (1992).
7. A. Pradel, V. M-Lledos, M. Ribes, and H. Eckert, *Solid State Ionics,* **53–56,** 1187 (1992).
8. C. A. Angell, *Ann. Rev. Phys. Chem.* **43,** 693 (1992).
9. A. Pradel and M. Ribes, *J. Non-Cryst. Solids* in press.
10. C. A. Angell, *Chem. Rev.* **90,** 523 (1990) and references therein.
11. C. A. Angell *in* "Relaxations in Complex Systems," K. L. Ngai and G. B. Wright, Eds), p. 203. National Technical Information Service, U.S. Department of Commerce, Springfield, VA, 1985.
12. (a) E. I. Kamitsos, A. P. Patsis, M. A. Karakassides and G. D. Chryssikos, *J. Non-Cryst. Solids* **126,** 52 (1990); (b) E. I. Kamitsos, A. P. Patsis, and G. D. Chryssikos, *J. Non-Cryst. Solids* **152,** 246 (1993).
13. G. Lukovsky, F. L. Galeener, R. C. Keezer, R. H. Geils, and H. A. Six, *Phys. Rev. B* **10,** 5134 (1974).
14. G. Lukovsky, J. P. de Neufville, and F. L. Galeener, *Phys. Rev. B* **9,** 1591 (1974).
15. P. M. Bridenbaugh, G. P. Espinsa, J. E. Griffiths, J. C. Phillips, and J. P. Remeika, *Phys. Rev. B* **20,** 4140 (1979).
16. K. Murase, T. Fukunaga, Y. Tanaka, K. Yakushiji, and I. Yunoki, *Physica B* **117 & 118,** 962 (1983).
17. P. Boolchand, J. Grothaus, M. Tenhover, M. A. Hazle, and R. K. Grasselli, *Phys. Rev. B* **33,** 5421 (1986).
18. K. Nakamoto, "Infrared and Raman Spectra of Inorganic and Coordination Compounds," p. 134. Wiley, New York, 1978.
19. L. Koudelka and M. Pisarcik, *J. Non-Cryst. Solids* **113,** 239 (1989).
20. T. Furukawa, K. E. Fox, and W. B. White, *J. Chem. Phys.* **75,** 3226 (1981).
21. P. McMillan, *Am. Miner.* **69,** 622 (1984).
22. E. I. Kamitsos, M. A. Karakassides, and G. D. Chryssikos, *J. Phys. Chem.* **91,** 5807 (1987).
23. E. I. Kamitsos, J. A. Kapoutsis, G. D. Chryssikos, and A. P. Patsis, *Bol. Soc. Esp. Ceram. Vid.* **31-C4,** 403 (1992).
24. E. I. Kamitsos, *J. Phys. Chem.* **93,** 1604 (1989).
25. G. Burns, F. H. Dacol, and M. W. Shafer, *Phys. Rev. B* **16,** 1416 (1977).
26. P. Bruesch, W. Buhrer, and H. J. M. Smeets, *Phys. Rev. B* **22,** 970 (1980).
27. U. Borges, G. Eckold, and K. Funke, *Ber. Bunsenges. Phys. Chem.* **82,** 702 (1978).
28. J. Wong and C. A. Angell, "Glass Structure by Spectroscopy," p. 750. Dekker, New York, 1976.
29. R. H. Cole and E. Tombari, *J. Non-Cryst. Solids* **131–133,** 969 (1991).
30. K. Funke, *Prog. Solid State Chem.* **22,** 111 (1993) and references therein.
31. P. Armand, A. Ibanez, H. Dexpert, D. B. Hencourt, D. Raoux, and E. Philippot, *J. Physi IV* **C2,** 189 (1992).
32. P. Armand, A. Ibanez, and E. Philippot, *J. Solid State Chem.* **104,** 308 (1993).